Shear-Induced Isotropic-Nematic Transition in Poly(Ether Ether Ketone) Melts

Daniele Parisi,[1] Jiho Seo,[1] Behzad Nazari,[2] Richard P. Schaake,[3] Alicyn M. Rhoades[2] and Ralph H. Colby[1]

[1]Department of Materials Science and Engineering, Penn State University, University Park, Pennsylvania 16802, United States.

[2]School of Engineering, Penn State Behrend, Erie, Pennsylvania 16563, United States.

[3]SKF Research & Technology Development, 3992 AE Houten, The Netherlands.

ABSTRACT

In a previous work on a poly(ether ether ketone) (PEEK) melt, above its nominal melting temperature ($T_m \cong 335$ °C), a severe Cox-Merz rule failure was observed. The abrupt decrease of the apparent shear viscosity was ascribed to the formation of Flow-Induced Crystallization (FIC) precursors. Here, shear rheology and reflection polariscope experiments are utilized to unravel the structural changes occurring under shear on a similar PEEK melt above T_m. Three regions of the flow curve were identified from low (0.01 s^{-1}) to high shear rates (1000 s^{-1}): I) isotropic structure with weak birefringence due to polymer chain orientation and mild shear thinning for $\dot{\gamma} < 1$ s^{-1}, II) isotropic-nematic transition accompanied by strong birefringence, two steady-state viscosities and large nematic polydomain director fluctuations and III) shear thinning behavior with a $\eta \sim \dot{\gamma}^{-0.5}$ dependence for $\dot{\gamma} > 20$ s^{-1}, typically found in nematic fluids. The findings reported in this experimental work suggest that the nematic phase may represent the early stage for the formation of shear-induced crystallization precursors.

Nematic fluids have always received a great deal of attention due to their rich opto-mechanical properties. A wide plethora of systems showing nematic phases has been investigated over the years, including rigid rods,[1–3] fd-viruses,[4,5] polymer-grafted nanocylinders[6,7] and liquid crystalline polymers.[8–11] The Isotropic-Nematic (I-N) transition promoted by shear is not sharp for polydisperse systems, but it can involve phase coexistence at different length scales (domains).[11–16] The resulting nematic phase, as in the case of liquid crystals subjected to shear, can be characterized by nematic director fluctuation and motion in the velocity direction, such as collective tumbling and wagging, or orientation in the vorticity direction, but motion in the velocity direction; log-rolling and kayaking.[9,14,17–20] These regimes are controlled by many factors: initial orientation of the system, polydispersity, interaction potential, aspect ratio, chain flexibility, domain composition and shear rate.[17,18,21,22] While the I-N transition promoted by shear has been extensively investigated in polymeric or colloidal solutions,[5,12,13,23,24] much less is known for polymer melts. Most of the literature refers to thermotropic melts.[14,15,21,25–29] Of considerable importance are the works of Beekmans et al.[25] who confirmed the presence of fluctuations in the stress and first normal stress differences in transient shear experiments, in situ X-ray scattering experiments of Rendon et al.[19] and by Romo-Uribe and Windle[14] probing tumbling and log-rolling, respectively, and Gotsis et al.[26] investigating the shear thinning regime of nematic melts with pressure-driven flows in capillary and slit dies. However, rheological evidences of a shear-induced I-N transition is still missing for polymer melts that never show a quiescent nematic phase.

In this Letter, we demonstrate that the poly(ether ether ketone) (PEEK) melt, sheared above its nominal melting temperature, exhibits an Isotropic-Nematic transition. The complex transient response of PEEK was unravelled by means of a combination of rheological and optical techniques, including shear rheology coupled with a reflection polariscope, cone partitioned plate rheometry and capillary rheometry.

PEEK 450G was purchased from Victrex (Lancashire, United Kingdom) and has a weight-average molecular weight M_w = 36.6 kg/mol with M_w/M_n = 2.9.[30] The Kuhn monomer length is b = 10.8 nm,[31] making PEEK a very stiff polymer compared to conventional semicrystalline polymers (b < 2 nm). The entanglement molecular weight was estimated to be 1500 g/mol,[32] yielding ~ 25 entanglements per chain for chains with $M = M_w$. Shear rheology experiments were performed in three different instruments: Anton Paar MCR 502 equipped with a 50 mm diameter transparent quartz bottom plate and an 8 mm diameter polished stainless steel top plate, enabling a reflection polariscope measuring birefringence in the velocity-vorticity plane;[33,34] Rheometrics Ares-LS equipped with a cone

partitioned plate[35] (6 mm inner plate diameter and 25 mm cone diameter with angle 0.04 rad and 53 nm truncation gap); and a Rosand dual-barrel capillary rheometer equipped with two dies, one is 30 mm length and the orifice is 0.25 mm in length, both with 1 mm diameter. All the experiments were performed at 370 °C, above the nominal melting temperature $T_m \cong 335$ °C[30] and below the equilibrium melting temperature of $T_m^0 \cong 380$ °C.[30] An annealing process of five minutes at 400 °C was applied after the loading, in order to erase the history of the sample.[36] 8 mm diameter disks, 0.8 mm thick were press-molded at 380 °C under nitrogen conditions inside a glove-box for twenty minutes.

Figure 1 shows the apparent viscosity and shear stress at 370 ºC as a function of shear rate at the perimeter of the parallel plate geometry, along with the complex viscosity as a function of frequency (see also Figure S1 in the SI). The birefringent images, also shown in Figure 1, refer to the velocity-vorticity plane and correspond to the red symbols in the flow curve. A shearing time of 30 s for each rate was chosen based on the steady-state attained with the lowest shear rate, $\dot{\gamma} = 0.01$ s^{-1}. As will be shown later, this does not always ensure steady-state conditions. Conveniently, the flow curve can be divided into three regimes which seem to differ from the picture of Asada-Onogi[37,38] and Marrucci-Grizzuti,[39] because there is no thinning regime at the probed low shear rate region, suggesting that the system is completely isotropic at rest and no nematic domains are present.

I) A Newtonian plateau at the lowest shear rates ($\dot{\gamma} < 0.1$ s^{-1}), indicating a zero-shear viscosity ~ 8000 Pa s, is characterized by very weak birefringence due to chain orientation along the flow direction (see Figure S2 in the SI). The Newtonian plateau is followed by mild shear thinning in Regime I, where the birefringence grows very slowly for $\dot{\gamma} < 1$ s^{-1}.

II) As the shear rate reaches 1 s^{-1}, an abrupt increase in birefringence was clearly observed (see birefringent image at $\dot{\gamma} = 1$ s^{-1} and Figure S2 in the SI), implying a significant structural change attributed to the I-N transition.[12,28,40] The border between Regimes I and II has a relaxation time corresponding to $1/\dot{\gamma} = 1$ s. This might represent the Rouse time τ_R of the longest chains, where such long chains get significantly stretched along the flow direction.[36,41] As $\dot{\gamma}$ increases, the failure of the Cox-Merz empirical rule[42] manifests. On a similar PEEK melt, sheared at 350 °C, Nazari et al.[36] assigned the failure of the Cox-Merz to the onset initiation of FIC precursors, with accelerated crystallization kinetics. In the range $1 < \dot{\gamma} < 20$ s^{-1} the failure of the Cox-Merz rule is accompanied by an abrupt drop in apparent viscosity with $\eta \sim \dot{\gamma}^{-1}$, implying flow instabilities. In fact, in this range of shear rates, the shear stress remains constant (~ 7000 Pa), typical of shear-banding. Berret et al.[12,13,43] witnessed an analogous rheological response in wormlike micelle

solutions, confirming an earlier prediction[44,45] on the nonlinear rheology of wormlike micelles, according to which the I-N transition is not sharp but rather characterized by two processes: nucleation and growth. During these processes, isotropic and nematic domains coexist, and their composition varies with $\dot{\gamma}$. We expect the shear rate in the nematic domains is much higher than in the isotropic domains, with different viscosity but the same shear stress, referred to as shear banding.[45–47]

III) For $\dot{\gamma}$ > 20 s^{-1} the entire sample is nematic, exhibiting a shear thinning regime with $\eta \sim \dot{\gamma}^{-0.5}$, as nematic phases seem to invariably display.[12,25,26,39,48–53]

The rich rheological response is accompanied by a remarkable evolution of birefringence Δn with shear rate and radial position (see images at 10, 30 and 100 s^{-1} in Figure 1). The birefringence is a measure of the optical anisotropy, resulting from the orientation and deformation of the chains in shear flow, seen as colored "fringes" in Figure 1. Note that isochromatic circular fringes correspond to regions where the normal stress differences are constant,[34] and their position shifts towards smaller radius as the shear rate at the perimeter increases. An elegant, yet effective, way to quantify birefringence follows.[33,34] First, a stack of images was created (see Figure 2A), each corresponding to a shear rate value of the flow curve reported in Figure 1. Second, a slicing plane at 45° to both the polarizer and the analyzer transmission planes[33,34] yields the birefringence spectrum as a function of radial position and the shear rate at the perimeter of the plate, shown in Figure 2B, along with the flow curve reported in Figure 1. The two white dashed lines in Figure 2B represent the iso-shear rate region at the I-N transition ($\dot{\gamma}$ = 1 s^{-1}). Lastly, the birefringent color observed at a given radial position is contrasted with the light path thickness (twice the measuring gap) in the Michel-Levy chart[54] to quantify the birefringence.

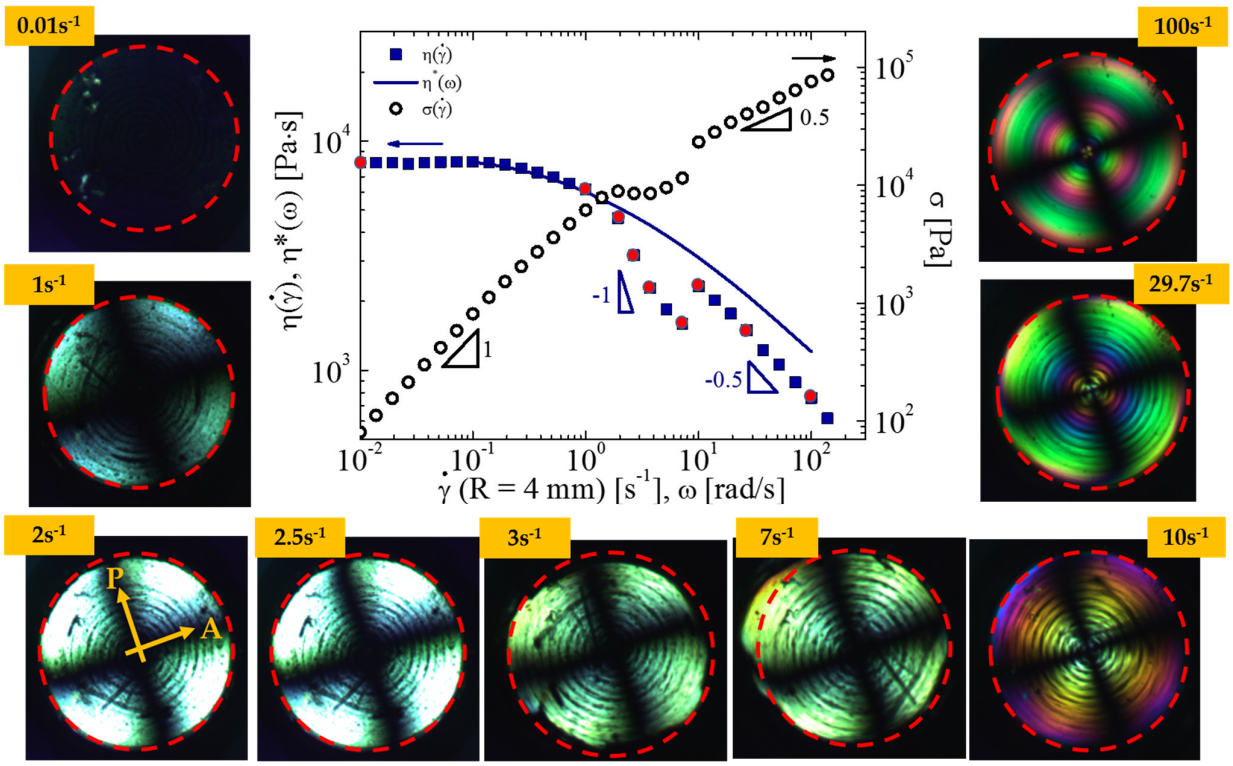

Figure 1. Apparent viscosity (blue symbols and left axis), complex viscosity (blue line and left axis) and shear stress (open black symbols and right axis) of PEEK 450G at 370 ºC, as a function of the shear rate at the perimeter of the plate geometry. Images are birefringence data at the nine shear rates indicated as red symbols. The rotational direction of the reflecting polished parallel plate is clockwise and the two yellow vectors in the birefringence image at 2 s^{-1}, labelled P and A, are the polarizer and the analyzer transmission azimuths, respectively. The shear rate in parallel plate geometry depends on the radial position as $\dot{\gamma} = \frac{\Omega r}{h}$, where Ω is the angular velocity, h is the measuring gap and r the radial position.

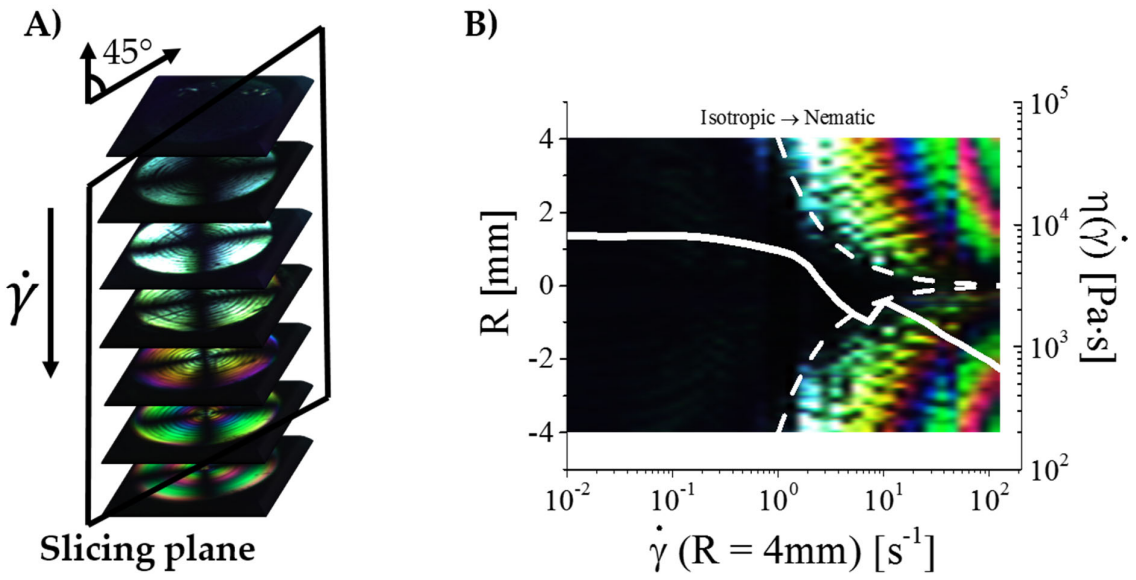

Figure 2. Birefringence data analysis for PEEK 450G at 370 ºC: A) The image at each plate rotation rate is sliced at 45º to both the polarizer and the analyzer transmission planes[34] and stacked to form the image in B) which also shows as white dashed lines, the 1 s^{-1} constant shear rate that corresponds to the isotropic-nematic transition and the apparent viscosity as a function of the shear rate at the perimeter of the sample (white solid line).

Figure 3 depicts the dependence of the birefringence on shear rate, both referred to the perimeter of the plate (R = 4 mm). Δn is positive in the whole range of shear rates, implying that PEEK flow aligns and the polarizability along the chain is larger than that perpendicular to the chain.[33,55] Analogous to the rheological response, the birefringence is divided into the same three regimes of shear rate. For $\dot{\gamma} < 1$ the magnitude of the birefringence is the lowest and only caused by chain orientation. In the range $1 < \dot{\gamma} < 20$ s^{-1} Δn shows a plateau when the system undergoes the I-N transition followed by an increase with $\dot{\gamma}$. In liquid crystalline solutions of poly(benzyl glutamate) and hydroxypropylcellulose, Hongladarom et al.[56–58] attributed the Δn plateau to tumbling and to net orientation imparted by polydomains in the Regime I defined in Refs. 37-39, respectively, whereas in the present case, the plateau is tentatively associated to the presence of shear bands, hence the coexistence of isotropic and nematic domains identified in Figure 1. A similar conjecture was also hypothesized by Noirez, et al.[27] in polydisperse liquid crystalline polymer melts. For $\dot{\gamma} > 20$ s^{-1} all the polymer chains contribute to the nematic phase and Δn increases as $\Delta n \sim \dot{\gamma}^{0.5}$, as reported by all studies of nematics that we are aware of.[28,29,56,59,60]

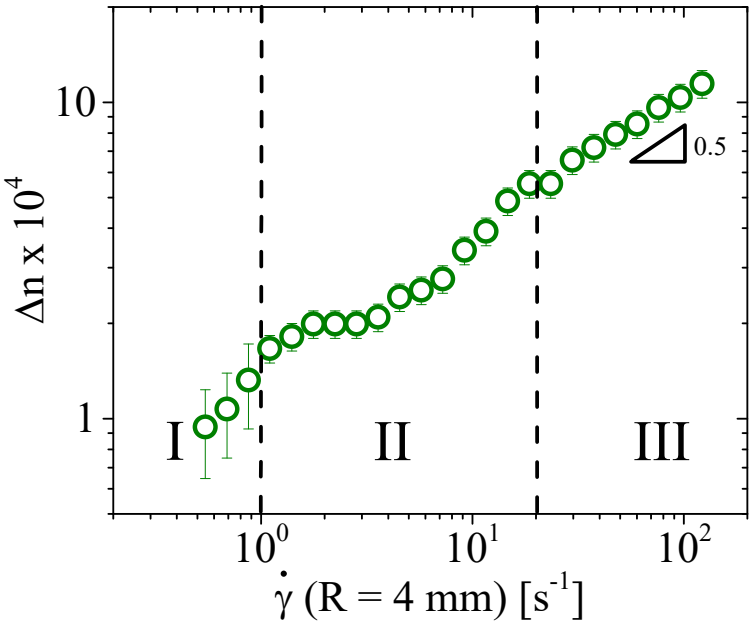

Figure 3. Birefringence Δn evaluated at R = 4 mm (perimeter of the plate) as a function of shear rate at the same radial position for PEEK 450G at 370 ºC. Error bars were estimated in terms of retardancy while reading the birefringent colors in the Michel-Levy chart.

We examined Regime II (the I-N transition) in detail via the start-up of shear at various shear rates, each time with a fresh sample, using a cone partitioned plate at 0.1, 1, 2, 3, 5, 10, 20 s^{-1}. In Regime III where the sample is presumably fully nematic, 30 and 40 s^{-1} also were studied but unfortunately higher shear rates could not be probed without edge fracture effects. A fresh disk was used for each $\dot{\gamma}$. The use of these tests with such a geometry has a threefold goal: 1) providing a uniform shear rate, 2) fixing to zero the shear history of the sample for each $\dot{\gamma}$ and 3) minimize edge fracture. The shearing time t was at least 1000 s for each $\dot{\gamma}$. Shear stress and primary normal stress difference as a function of strain ($\gamma = \dot{\gamma}t$) are presented in Figures 4A and 4B, respectively. Three important findings are: 1) Two steady-states in the range $1 < \dot{\gamma} < 20$ s^{-1}, one occurring at ~ 20 strain units, and a second one at ~ 2000 strain units. While the first steady-state is assigned to the response of the isotropic phase, the second one with lower apparent viscosity is attributed to the nematic/isotropic biphase, where two bands coexist with the same shear stress. Presumably the long chains are in the nematic domains and the shorter chains are still isotropic. As shear rate increases, more chains join the nematic domains. 2) The second steady-state is characterized by uncorrelated fluctuations in the shear stress (or in N_1) that are attributed to fluctuations of the polydomain nematic directors, known as wagging.[9,18,20] 3) At $\dot{\gamma} > 20$ s^{-1} the two steady-states merge into one single steady-state.

Ugaz and Burghardt[61] proposed a simplified version of the Leslie-Ericksen theory[62] that studies the evolution of anisotropy of polydomains and shear stress during a start-up of shear flow in thermotropic polymers. On the assumption of negligible elastic distortions,[61] the orientation response depends on a single material constant, the tumbling parameter λ. Flow aligning dynamics are expected for $\lambda > 1$ whereas $\lambda < 1$ reflects tumbling. In flow aligning ($\lambda > 1$) liquid crystal polymers, the tumbling parameter solely depends on mechanical data[63] by knowing the steady-state conditions of the first normal stress difference N_1 and the shear stress σ: $\frac{N_1}{\sigma} = \frac{2}{\sqrt{\lambda^2-1}}$. (see inset in Figure 4C). Assuming only flow alignment, supported by the positive sign of Δn, data of N_1 and σ reported in Figures 4A and 4B were used to calculate the shear rate dependence of λ as is shown in Figure 4C (green symbols). λ was found to decrease with increasing shear rate, pointing towards the trend exhibited by semiflexible chains with increasing order parameter,[64] a result which is in good agreement with the pronounced chain rigidity of PEEK. The tumbling parameter λ is also related to director orientation angle, relative to the flow direction:[64] $tan\theta = \sqrt{\frac{\lambda-1}{\lambda+1}}\tanh\left(\frac{\gamma}{2}\sqrt{\lambda^2-1}\right)$,where γ is the shear strain. As λ becomes smaller, θ decreases as well, until $\lambda = 1$ and $\theta = 0$ for a perfectly shear-aligned system. In the present case, by using the strain corresponding to the nematic phase (2000 strain units) θ decreases from 35° to a steady orientation of 20° with increasing shear rate, as reported in Figure 4C (black symbols and right axis).

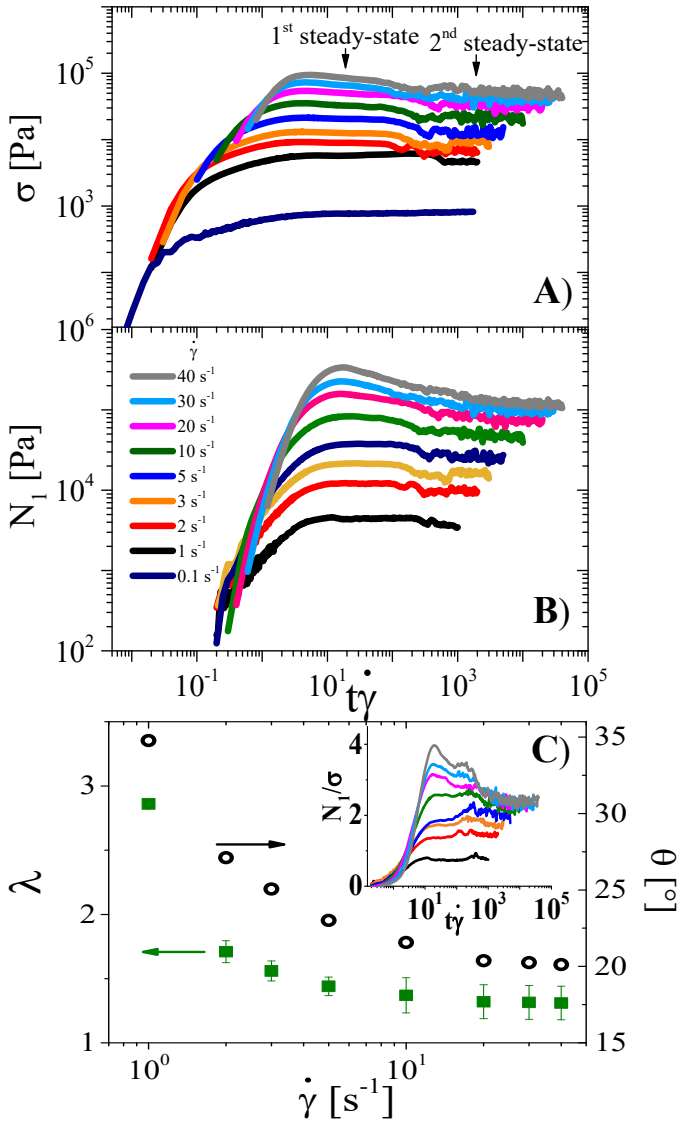

Figure 4. Start-up of shear at 370 °C for fresh loadings of PEEK450G using the cone-partitioned plate in terms of A) shear stress σ and B) primary normal stress difference N_1 as a function of shear strain. Panel C) shows the shear rate dependence of the tumbling parameter λ (green symbols - left axis) and the director orientation angle θ, relative to the flow direction (black symbols - right axis) for PEEK 450G at 370 °C. Error bars for λ refer to the standard deviation of the mean steady-state values of the $\frac{N_1}{\sigma}$ ratio. The black arrows in panel A indicate the first steady state at γ = 20 (isotropic response) and the second steady-state at γ = 2000 (nematic response). N_1 at 0.1 s^{-1} is not reported because the normal force was below the transducer resolution limit. The inset in panel C displays the $\frac{N_1}{\sigma}$ ratio as a function of shear strain at various shear rates reported in the legend of panel B.

In view of the results presented in Figure 4, it is possible to create a more refined flow curve as reported in Figure 5. The apparent viscosity shown in Figure 1 appears now as a solid black line. The apparent viscosity values, calculated from the first and second steady-states of Figure 4A ($\eta = \sigma/\dot{\gamma}$)

are displayed as red and blue open circles, respectively. Interestingly, the apparent viscosity calculated from the first steady-state aligns perfectly with the complex viscosity, validating the empirical Cox-Merz rule. This represents the isotropic response. $\dot{\gamma}$ = 1 s^{-1} marks the lowest shear rate at which two steady-states are observed; the I-N transition. The blue circles represent the "true" steady-state apparent viscosity values of the shear-banded biphase where the high molecular weight chains presumably form a nematic phase that coexists with an isotropic phase comprising lower molecular weight chains. In fact, the lower apparent viscosity values in the range $4 < \dot{\gamma} < 8$ s^{-1}, measured with a fixed shearing time, might not represent steady-state values (see gray region in Figure 5 and Figure S3 in the SI) as it was not known, a priori, the existence of a second steady-state. This occurs in Regime II, where fluctuations in viscosity are also quite significant (see Figure S3 in the SI). A very good agreement between the two sets of data is then recovered at $\dot{\gamma}$ >10 s^{-1}, where the system response starts being dominated only by the nematic phase and the two steady-states start to merge. Note that $\dot{\gamma}$ = 20 s^{-1} represents the highest rate at which it is still possible to measure a transient isotropic response. For $\dot{\gamma} > 20$ s^{-1}, only a fully nematic response is obtained (Regime III). Finally, rheology of PEEK in Poiseuille flow (blue squares in Fig. 5) validated the shear thinning Regime III at $\dot{\gamma} > 20$ s^{-1} with $\eta \sim \dot{\gamma}^{-0.5}$, and extended the flow curve by more than a decade in shear rate.

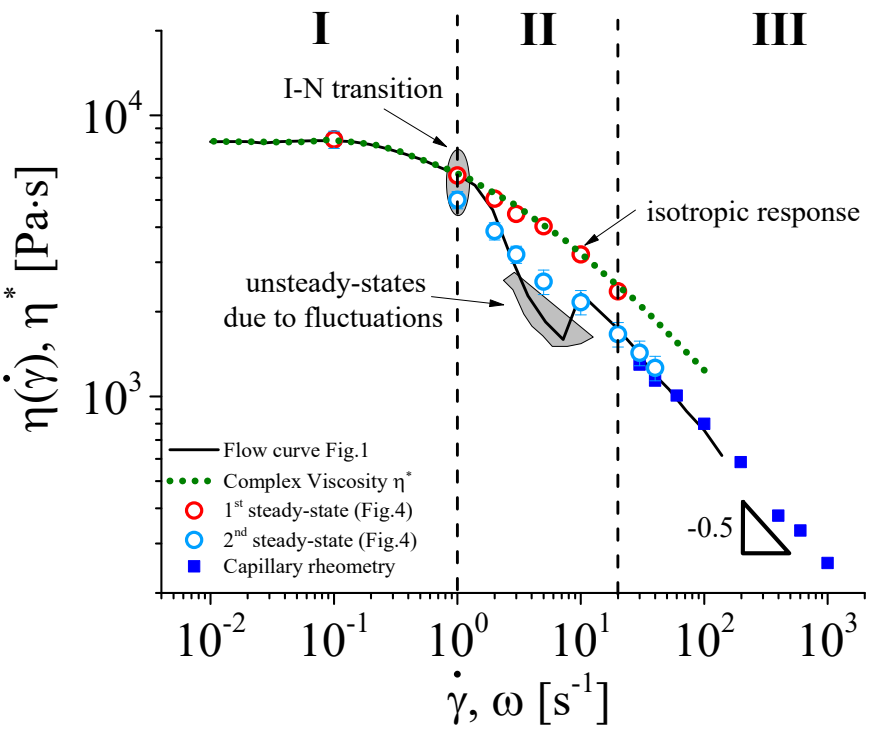

Figure 5. Apparent steady state and complex viscosities as a function of shear rate and frequency, respectively, for PEEK 450G at 370 ºC. The black line represents the flow curve reported in Figure 1. The green dotted line is the complex viscosity (see blue symbols in Figure S1). Red and blue circles are steady-state viscosities estimated from the first and second steady-state plateau shown in Figure 4A. Blue squares are viscosity values obtained with capillary rheometry at 370 °C. The gray region at 1 s^{-1} corresponds to the I-N transition of the longest chains that get stretched in the shear flow, whereas the one between 2 s^{-1} and 6 s^{-1} refers to strong fluctuations in the nematic/isotropic biphase (see figure S3 in the SI). Vertical black dashed lines mark Regimes I, II and III (see text).

In light of the refined results displayed in Figure 5 the following scenario is thus proposed, assuming that the 1 s^{-1} shear rate where Regime II starts is the reciprocal of the Rouse time of the longest chains, $\tau_R = 1$ s.

For $\dot{\gamma}\tau_R < 1$ the system is only isotropic, regardless of the shearing time. At $\dot{\gamma}\tau_R = 1$, the longest chains of the system get stretched, and the isotropic response is then followed by the nematic nucleation as the shearing time (or strain) increases. The two responses are well decoupled in time (or strain) reflected in the presence of two steady-states in the transient response. In Regime II, the nematic phase forms domains (or bands), within which the longest chains are oriented and stretched, surrounded by an isotropic phase of shorter chains that are only oriented. The nematic phase is now characterized by uncorrelated time fluctuations of the shear stress that increase with $\dot{\gamma}$. As shear rate increases in Regime II, more chains get stretched to join the nematic domains. Thus far, the isotropic

response complies with the complex viscosity, fulfilling the Cox-Merz Rule. For $\dot{\gamma}\tau_R > 20$ (Regime III) all chains are nematic. As the shear flow starts, all the chains start immediately to flow align, smearing out the isotropic response. Rotational and capillary rheometry agree well, yielding $\eta \sim \dot{\gamma}^{-0.5}$, reflecting the shear thinning of all nematic fluids.[12,25,26,39,48]

The stress-optical rule correlates the birefringence with the primary (N_1) and secondary (N_2) normal stress differences as $\Delta n = CN_1(N_2/N_1+1)$ with C being the stress-optical coefficient.[34] Assuming that N_2 is negligible compared to N_1, $\Delta n = CN_1$ is obtained. The latter enables the estimation of the stress-optical coefficient by knowing Δn from the reflection polariscope and N_1 from Figure 4B. Figure 6A shows the birefringence as a function of radial position and strain ($\gamma = \dot{\gamma}t$) obtained with a start-up of shear experiment at $\dot{\gamma}$ = 30 s^{-1} (at the perimeter of the plate). The strain units related to the two steady states are also displayed as vertical black dashed lines. By using the Michel-Levy chart, birefringence values were calculated at different radial positions, 4 mm, 2.7 mm, 1.3 mm, 0.7 mm, corresponding to shear rate values of 30 s^{-1}, 20 s^{-1}, 10 s^{-1}, 5 s^{-1}, respectively. Such values were then contrasted to those of N_1 reported in Figure 4B, therefore, the stress optical coefficient was calculated in the two steady-states and displayed in Figure 6B. The stress-optical coefficient takes values between 5.65×10^{-9} and 5.95×10^{-9} Pa^{-1} regardless of the shear rate and the steady-state which is referred to. In fact, the stress-optical coefficient is directly proportional to the difference between the parallel and perpendicular polarizabilty of a Kuhn segment,[65] or analogously, to the chain rigidity.[66] Thus, as PEEK is characterized by a large Kuhn length (b = 10.8 nm)[31] and a linear molecular structure, the parallel polarizability is much larger than the perpendicular polarizability, resulting in a positive stress optical coefficient ~ 5.8×10^{-9} Pa^{-1} that is considerably larger than more flexible polymers,[65] such as isotactic polypropylene (C ~ 0.9×10^{-9} Pa^{-1}, b = 1.1 nm), polyisoprene (C ~ 1.9×10^{-9} Pa^{-1}, b < 1 nm), polyethylene (C ~ 2.5×10^{-9} Pa^{-1}, b = 1.4 nm), polybutadiene (C ~ 3.3×10^{-9} Pa^{-1}, b = 1.0 nm) and polystyrene (C ~ -4.5×10^{-9} Pa^{-1}, b = 1.8 nm).

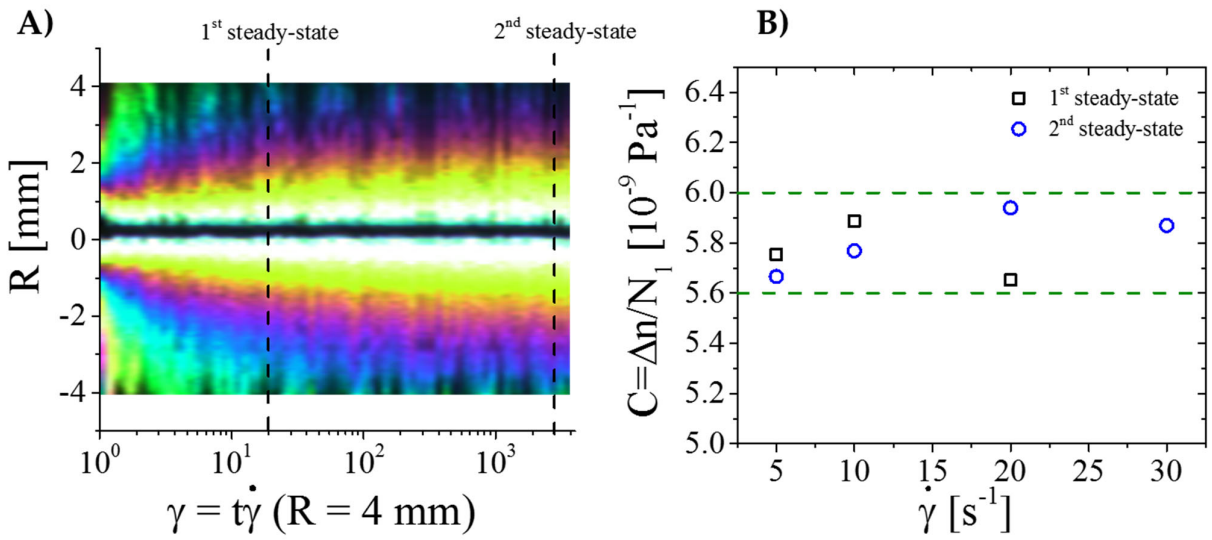

Figure 6. A) Slice of the stack of shear-induced polarized light images (sliced by a plane at 45° to both the polarizer and the analyzer transmission planes)[34] during a start-up of shear at $\dot{\gamma}$ = 30 s^{-1} at the perimeter of the plate. Birefringence as a function of radial position and shear strain at the perimeter of the plate is obtained. The two vertical dashed lines indicate the two steady-states (see text). B) Stress optical coefficient estimated as $C=\Delta n/N_1$ at various radial positions (or $\dot{\gamma}$) reported in panel A: 30 s^{-1} R = 4 mm, 20 s^{-1} R = 2.7 mm, 10 s^{-1} R =1.3 mm, 5 s^{-1} R = 0.7 mm. N_1 values refer to Figure 4. The value of the stress optical coefficient falls in the range $5.65 \times 10^{-9} < C < 5.95 \times 10^{-9}$ Pa^{-1} (see horizontal dashed lines).

The entangled rigid PEEK melt exhibits an isotropic-nematic transition, promoted by shear flow. The PEEK transient shear response is complex, suggesting multiple structural changes. Conveniently, three regimes were identified by means of different rheological and optical techniques: I) an isotropic regime with weak chain orientation at low shear rates, II) an I-N transition where isotropic and nematic phases, well separated in the time (or strain), coexist and their compositions depend on shear rate $\dot{\gamma}$, and III) a shear thinning regime at high shear rates, where the whole system is nematic and the viscosity decreases as $\eta \sim \dot{\gamma}^{-0.5}$.[12,25,26,39,48] We hypothesize that formation of the nematic phase in shear may play an important role in flow-induced crystallization.[36,67]

ASSOCIATED CONTENT

SUPPORTING INFORMATION

Small Amplitude Oscillatory Shear in terms of dynamic moduli G′ and G″, and complex viscosity η^* as a function of oscillation frequency; apparent viscosity as a function of shear rate and shear-induced polarized light images.

AUTHOR INFORMATION

CORRESPONDING AUTHOR

Ralph. H. Colby - Department of Materials Science and Engineering, Penn State University, University Park, Pennsylvania 16802, United States
Email: rhc@plmsc.psu.edu

ORCID

Daniele Parisi: 0000-0002-1650-8429

Jiho Seo: 0000-0001-9374-4591

Behzad Nazari: 0000-0002-9106-5445

Alicyn M. Rhoades: 0000-0003-4678-419X

Ralph H. Colby: 0000-0002-5492-6189

NOTES

The authors declare no competing financial interest.

ACKNOWLEDGMENTS

This research was funded by SKF.

REFERENCES

(1) Buining, P. A.; Lekkerkerker, H. N. W. Isotropic-Nematic Phase Separation of a Dispersion of Organophilic Boehmite Rods. *The Journal of Physical Chemistry* **1993**, *97* (44), 11510–11516.

(2) Lekkerkerker, H. N. W.; Vroege, G. J. Liquid Crystal Phase Transitions in Suspensions of Mineral Colloids: New Life from Old Roots. *Philosophical Transactions of the Royal Society A: Mathematical, Physical and Engineering Sciences* **2013**, *371* (1988), 20120263.

(3) Solomon, M. J.; Spicer, P. T. Microstructural Regimes of Colloidal Rod Suspensions, Gels, and Glasses. *Soft Matter* **2010**, *6* (7), 1391.

(4) Lettinga, M. P.; Kang, K.; Holmqvist, P.; Imhof, A.; Derks, D.; Dhont, J. K. Nematic-Isotropic Spinodal Decomposition Kinetics of Rodlike Viruses. *Physical Review E* **2006**, *73* (1), 011412.

(5) Lettinga, M. P.; Dogic, Z.; Wang, H.; Vermant, J. Flow Behavior of Colloidal Rodlike Viruses in the Nematic Phase. *Langmuir* **2005**, *21* (17), 8048–8057.

(6) Zhang, Z.; Krishna, N.; Lettinga, M. P.; Vermant, J.; Grelet, E. Reversible Gelation of Rod-like Viruses Grafted with Thermoresponsive Polymers. *Langmuir* **2009**, *25* (4), 2437–2442.

(7) Parisi, D.; Ruan, Y.; Ochbaum, G.; Silmore, K. S.; Cullari, L.; Liu, C.-Y.; Bitton, R.; Regev, O.; Swan, J. W.; Loppinet, B. Short and Soft: Multi-Domain Organization, Tunable Dynamics and Jamming in Suspensions of Grafted Colloidal Cylinders with Small Aspect Ratio. *Langmuir* **2019**.

(8) Grosso, M.; Crescitelli, S.; Somma, E.; Vermant, J.; Moldenaers, P.; Maffettone, P. L. Prediction and Observation of Sustained Oscillations in a Sheared Liquid Crystalline Polymer. *Physical review letters* **2003**, *90* (9), 098304.

(9) Mewis, J.; Mortier, M.; Vermant, J.; Moldenaers, P. Experimental Evidence for the Existence of a Wagging Regime in Polymeric Liquid Crystals. *Macromolecules* **1997**, *30* (5), 1323–1328.

(10) Vermant, J.; Moldenaers, P.; Picken, S. J.; Mewis, J. A Comparison between Texture and Rheological Behaviour of Lyotropic Liquid Crystalline Polymers during Flow. *Journal of non-newtonian fluid mechanics* **1994**, *53*, 1–23.

(11) Srinivasarao, M. Rheology and Rheo-Optics of Polymer Liquid Crystals. *International Journal of Modern Physics B* **1995**, *9* (18n19), 2515–2572.

(12) Berret, J.-F.; Roux, D. C.; Porte, G. Isotropic-to-Nematic Transition in Wormlike Micelles under Shear. *Journal de Physique II* **1994**, *4* (8), 1261–1279.

(13) Berret, J.-F.; Roux, D. C.; Porte, G.; Lindner, P. Shear-Induced Isotropic-to-Nematic Phase Transition in Equilibrium Polymers. *EPL (Europhysics Letters)* **1994**, *25* (7), 521.

(14) Romo-Uribe, A.; Windle, A. H. "Log-Rolling" Alignment in Main-Chain Thermotropic Liquid Crystalline Polymer Melts under Shear: An In-Situ WAXS Study. *Macromolecules* **1996**, *29* (19), 6246–6255.

(15) Romo-Uribe, A.; Windle, A. H. A Flow-Orientation Transition in a Thermotropic Random Copolyester. *Macromolecules* **1993**, *26* (25), 7100–7102.

(16) Onogi, Y.; White, J. L.; Fellers, J. F. Structural Investigations of Polymer Liquid-Crystalline Solutions: Aromatic Polyamides, Hydroxy Propyl Cellulose, and Poly (γ-Benzyl-L-Glutamate). *Journal of Polymer Science: Polymer Physics Edition* **1980**, *18* (4), 663–682.

(17) Tao, Y.-G.; den Otter, W. K.; Briels, W. J. Periodic Orientational Motions of Rigid Liquid-Crystalline Polymers in Shear Flow. *The Journal of chemical physics* **2006**, *124* (20), 204902.

(18) Tao, Y.-G.; den Otter, W. K.; Briels, W. J. Kayaking and Wagging of Rods in Shear Flow. *Physical review letters* **2005**, *95* (23), 237802.

(19) Rendon, S.; Burghardt, W. R.; Bubeck, R. A. Orientation Dynamics in Commercial Thermotropic Liquid Crystalline Polymers in Transient Shear Flows. *Rheologica Acta* **2007**, *46* (7), 945–956.

(20) Tao, Y.-G.; den Otter, W. K.; Briels, W. J. Kayaking and Wagging of Liquid Crystals under Shear: Comparing Director and Mesogen Motions. *EPL (Europhysics Letters)* **2009**, *86* (5), 56005.

(21) Beekmans, F.; Gotsis, A. D.; Norder, B. Influence of the Flow History on Stress Growth and Structure Changes in the Thermotropic Liquid Crystalline Polymer Vectra B950. *Rheologica Acta* **1997**, *36* (1), 82–95.

(22) Forest, M. G.; Zhou, R.; Wang, Q. Full-Tensor Alignment Criteria for Sheared Nematic Polymers. *Journal of Rheology* **2003**, *47* (1), 105–127.

(23) Kannan, R. M.; Kornfield, J. A.; Schwenk, N.; Boeffel, C. Rheology of Side-Group Liquid-Crystalline Polymers: Effect of Isotropic-Nematic Transition and Evidence of Flow Alignment. *Macromolecules* **1993**, *26* (8), 2050–2056.

(24) Roux, D. C.; Berret, J.-F.; Porte, G.; Peuvrel-Disdier, E.; Lindner, P. Shear-Induced Orientations and Textures of Nematic Living Polymers. *Macromolecules* **1995**, *28* (5), 1681–1687.

(25) Beekmans, F.; Gotsis, A. D.; Norder, B. Transient and Steady-state Rheological Behavior of the Thermotropic Liquid Crystalline Polymer Vectra B950. *Journal of Rheology* **1996**, *40* (5).

(26) Gotsis, A. D.; Langelaan, H. C. Origins of Nonlinear Pressure Profiles in the Flow of Nematic Melts in Capillaries and Slits. *Journal of Rheology* **1994**, *38* (5), 1369–1383.

(27) Mendil-Jakani, H.; Baroni, P.; Noirez, L. Shear-Induced Isotropic to Nematic Transition of Liquid-Crystal Polymers: Identification of Gap Thickness and Slipping Effects. *Langmuir* **2009**, *25* (9), 5248–5252.

(28) Noirez, L. Origin of Shear-Induced Phase Transitions in Melts of Liquid-Crystal Polymers. *Physical Review E* **2005**, *72* (5), 051701.

(29) Mendil, H.; Baroni, P.; Noirez, L. Unexpected Giant Elasticity in Side-Chain Liquid-Crystal Polymer Melts: A New Approach for the Understanding of Shear-Induced Phase Transitions. *EPL (Europhysics Letters)* **2005**, *72* (6), 983.

(30) Seo, J.; Gohn, A. M.; Dubin, O.; Takahashi, H.; Hasegawa, H.; Sato, R.; Rhoades, A. M.; Schaake, R. P.; Colby, R. H. Isothermal Crystallization of Poly (Ether Ether Ketone) with Different Molecular Weights over a Wide Temperature Range. *Polymer Crystallization* **2019**, *2* (1), e10055.

(31) Bishop, M. T.; Karasz, F. E.; Russo, P. S.; Langley, K. H. Solubility and Properties of a Poly (Aryl Ether Ketone) in Strong Acids. *Macromolecules* **1985**, *18* (1), 86–93.

(32) Fetters, L. J.; Lohse, D. J.; Richter, D.; Witten, T. A.; Zirkel, A. Connection between Polymer Molecular Weight, Density, Chain Dimensions, and Melt Viscoelastic Properties. *Macromolecules* **1994**, *27* (17), 4639–4647.

(33) Mykhaylyk, O. O.; Warren, N. J.; Parnell, A. J.; Pfeifer, G.; Laeuger, J. Applications of Shear-Induced Polarized Light Imaging (SIPLI) Technique for Mechano-Optical Rheology of Polymers and Soft Matter Materials. *Journal of Polymer Science Part B: Polymer Physics* **2016**, *54* (21), 2151–2170.

(34) Mykhaylyk, O. O. Time-Resolved Polarized Light Imaging of Sheared Materials: Application to Polymer Crystallization. *Soft Matter* **2010**, *6* (18), 4430–4440.

(35) Costanzo, S.; Huang, Q.; Ianniruberto, G.; Marrucci, G.; Hassager, O.; Vlassopoulos, D. Shear and Extensional Rheology of Polystyrene Melts and Solutions with the Same Number of Entanglements. *Macromolecules* **2016**, *49* (10), 3925–3935.

(36) Nazari, B.; Rhoades, A. M.; Schaake, R. P.; Colby, R. H. Flow-Induced Crystallization of Peek: Isothermal Crystallization Kinetics and Lifetime of Flow-Induced Precursors during Isothermal Annealing. *ACS Macro Letters* **2016**, *5* (7), 849–853.

(37) Asada, T.; Toda, K.; Onogi, S. Deformation and Structural Re-Formation of Lyotropic Cholesteric Liquid Crystal of Hydroxypropyl Cellulose+ Water System. *Molecular Crystals and Liquid Crystals* **1981**, *68* (1), 231–246.

(38) Onogi, S.; Asada, T. Rheology and Rheo-Optics of Polymer Liquid Crystals. In *Rheology*; Springer, **1980**; pp 127–147.

(39) Marrucci, G.; Grizzuti, N. Rheology of Liquid-Crystalline Polymers. Theory and Experiments. *Makromolekulare Chemie. Macromolecular Symposia* **1991**, *48–49* (1), 181–188.

(40) Mather, P. T.; Romo-Uribe, A.; Han, C. D.; Kim, S. S. Rheo-Optical Evidence of a Flow-Induced Isotropic- Nematic Transition in a Thermotropic Liquid-Crystalline Polymer. *Macromolecules* **1997**, *30* (25), 7977–7989.

(41) Seo, J.; Gohn, A. M.; Schaake, R. P.; Parisi, D.; Rhoades, A. M.; Colby, R. H. Shear Flow-Induced Crystallization of Poly (Ether Ether Ketone). *Macromolecules* **2020**.

(42) Cox, W. P.; Merz, E. H. Correlation of Dynamic and Steady Flow Viscosities. *Journal of Polymer Science* **1958**, *28* (118), 619–622.

(43) Berret, J.-F. Rheology of Wormlike Micelles: Equilibrium Properties and Shear Banding Transitions. In *Molecular gels*; Springer, 2006; pp 667–720.

(44) Spenley, N. A.; Cates, M. E.; McLeish, T. C. B. Nonlinear Rheology of Wormlike Micelles. *Physical review letters* **1993**, *71* (6), 939.

(45) Fielding, S. M.; Olmsted, P. D. Flow Phase Diagrams for Concentration-Coupled Shear Banding. *The European Physical Journal E* **2003**, *11* (1), 65–83.

(46) Fielding, S. M.; Olmsted, P. D. Kinetics of the Shear Banding Instability in Startup Flows. *Physical Review E* **2003**, *68* (3), 036313.

(47) Olmsted, P. D. Perspectives on Shear Banding in Complex Fluids. *Rheologica Acta* **2008**, *47* (3), 283–300.

(48) Marrucci, G. Remarks on the Viscosity of Polymeric Liquid Crystals. *Advances in rheology* **1984**, *1*.

(49) Gillmor, J. R.; Colby, R. H.; Hall, E.; Ober, C. K. Viscoelastic Properties of a Model Main-Chain Liquid Crystalline Polyether. *Journal of Rheology* **1994**, *38* (5), 1623–1638.

(50) Fox, R. J.; Forest, M. G.; Picken, S. J.; Dingemans, T. J. Observation of Transition Cascades in Sheared Liquid Crystalline Polymers. *Soft Matter* **2020**.

(51) Hu, Y. T.; Boltenhagen, P.; Pine, D. J. Shear Thickening in Low-Concentration Solutions of Wormlike Micelles. I. Direct Visualization of Transient Behavior and Phase Transitions. *Journal of Rheology* **1998**, *42* (5), 1185–1208.

(52) Larson, R. G. The Structure and Rheology of Complex Fluids. 1999. *New York: Oxford* **1999**, *688*.

(53) Zhou, W.-J.; Kornfield, J. A.; Ugaz, V. M.; Burghardt, W. R.; Link, D. R.; Clark, N. A. Dynamics and Shear Orientation Behavior of a Main-Chain Thermotropic Liquid Crystalline Polymer. *Macromolecules* **1999**, *32* (17), 5581–5593.

(54) Bloss, F. D. *Optical Crystallography*; Mineralogical Society of America, 1999; Vol. 5.

(55) Stein, R. S.; Finkelstein, R. S. Optical Properties of Polymers. *Annual Review of Physical Chemistry* **1973**, *24* (1), 207–234.

(56) Hongladarom, K.; Secakusuma, V.; Burghardt, W. R. Relation between Molecular Orientation and Rheology in Lyotropic Hydroxypropylcellulose Solutions. *Journal of Rheology* **1994**, *38* (5), 1505–1523.

(57) Hongladarom, K.; Burghardt, W. R.; Baek, Sg.; Cementwala, S.; Magda, J. J. Molecular Alignment of Polymer Liquid Crystals in Shear Flows. 1. Spectrographic Birefringence Technique, Steady-State Orientation, and Normal Stress Behavior in Poly (Benzyl Glutamate) Solutions. *Macromolecules* **1993**, *26* (4), 772–784.

(58) Hongladarom, K.; Burghardt, W. R. Molecular Alignment of Polymer Liquid Crystals in Shear Flows. 2. Transient Flow Behavior in Poly (Benzyl Glutamate) Solutions. *Macromolecules* **1993**, *26* (4), 785–794.

(59) Mather, P. T.; Jeon, H. G.; Han, C. D.; Chang, S. Odd- Even Effect of Flexible Spacer Length on Flow-Induced Isotropic-to-Nematic Transition in Segmented Thermotropic Polymers. *Macromolecules* **2002**, *35* (4), 1326–1335.

(60) Bailey, C.; Fodor-Csorba, K.; Verduzco, R.; Gleeson, J. T.; Sprunt, S.; Jakli, A. Large Flow Birefringence of Nematogenic Bent-Core Liquid Crystals. *Physical review letters* **2009**, *103* (23), 237803.

(61) Ugaz, V. M.; Burghardt, W. R. In Situ X-Ray Scattering Study of a Model Thermotropic Copolyester under Shear: Evidence and Consequences of Flow-Aligning Behavior. *Macromolecules* **1998**, *31* (24), 8474–8484.

(62) De Gennes, P.-G.; Prost, J. *The Physics of Liquid Crystals*; Oxford university press, 1993; Vol. 83.

(63) Ugaz, V. M.; Burghardt, W. R.; Zhou, W.; Kornfield, J. A. Transient Molecular Orientation and Rheology in Flow Aligning Thermotropic Liquid Crystalline Polymers. *Journal of Rheology* **2001**, *45* (5), 1029–1063.

(64) Zhou, W.-J.; Kornfield, J. A.; Burghardt, W. R. Shear Aligning Properties of a Main-Chain Thermotropic Liquid Crystalline Polymer. *Macromolecules* **2001**, *34* (11), 3654–3660.

(65) Buning, G. W.; Wimberger-Friedl, R.; Janeschitz-Kriegl, H.; Ford, T. M. Optical Anisotropy of Polycarbonates. In *Integration of Fundamental Polymer Science and Technology—2*; Springer, 1988; pp 405–409.

(66) Liang, T.; Takahara, A.; Saito, K.; Kajiyama, T. Effects of Main Chain Rigidity on Nonlinear Dynamic Viscoelasticity and Fatigue Performance for Polymeric Fibres. *Polymer* **1998**, *39* (22), 5387–5392.

(67) Nicholson, D. A.; Rutledge, G. C. Flow-Induced Inhomogeneity and Enhanced Nucleation in a Long Alkane Melt. *Polymer* **2020**, *200*, 122605.

ToC Graphic:

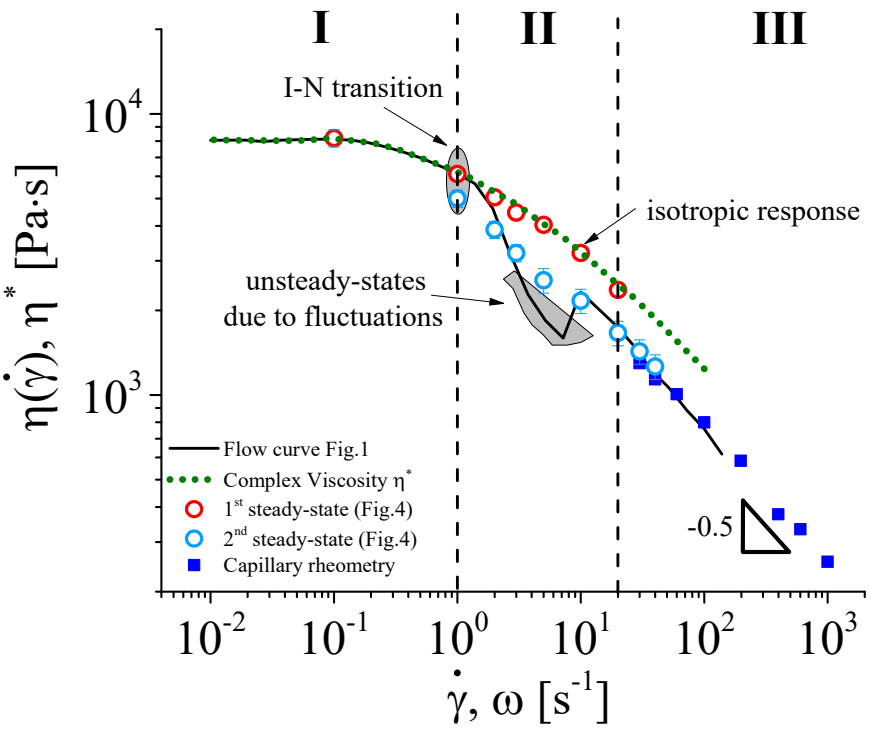

SUPPORTING INFORMATION

Shear-Induced Isotropic-Nematic Transition in Poly(Ether Ether Ketone) Melts

Daniele Parisi,[1] Jiho Seo,[1] Behzad Nazari,[2] Richard P. Schaake,[3] Alicyn M. Rhoades[2] and Ralph H. Colby*[1]

[1]Department of Materials Science and Engineering, Penn State University, University Park, Pennsylvania 16802, United States.

[2]School of Engineering, Penn State Behrend, Erie, Pennsylvania 16563, United States.

[3]SKF Research & Technology Development, 3992 AE Houten, The Netherlands.

*Corresponding author: rhc@plmsc.psu.edu

S1. Linear Viscoelasticity: Small Amplitude Oscillatory Shear

Figure S1 shows the linear viscoelastic spectrum in terms of dynamic moduli G′ and G″, and complex viscosity η^* as functions of oscillation frequency for PEEK 450G at 370 °C. Data were obtained with a rotational rheometer Anton Paar MCR 502 equipped with a 50 mm diameter transparent quartz bottom plate and an 8 mm diameter polished stainless steel top plate. Measurements performed at 370 °C were preceded by a five minutes annealing process at 400 °C to erase the mechanical history of the sample.[1]

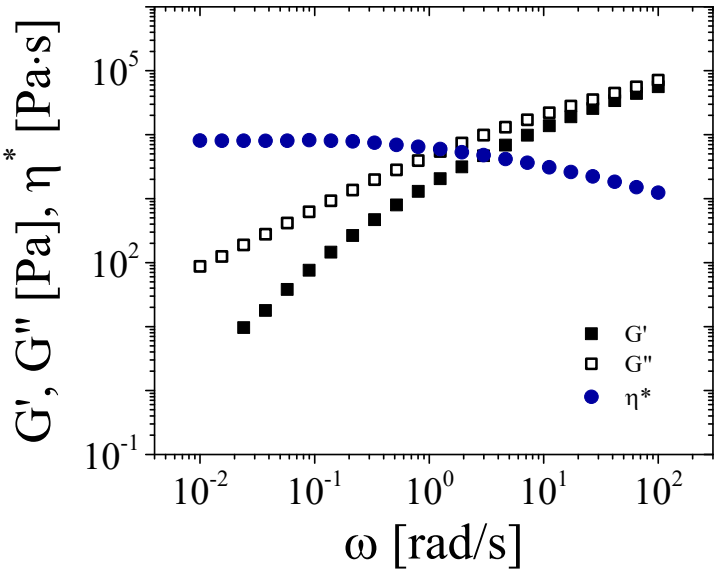

Figure S1. Dynamic moduli G′ (solid symbols), G″ (open symbols) and complex viscosity η^* (blue symbols) as functions of oscillation frequency for PEEK 450G at 370 °C.

S2. Reflection Polariscope: Shear-Induced Polarized Light Images

Figure S2 complements the birefringent images shown in Figure 1, in the main text. Images refer to the velocity-vorticity plane. While for $\dot{\gamma} < 1\ s^{-1}$ the birefringence is rather weak and caused only by chain orientation, a clear increase is detectable at $\dot{\gamma} = 1\ s^{-1}$, at the Isotropic-Nematic transition. Note that, at $\dot{\gamma} = 1\ s^{-1}$ the "Maltese cross" manifests. When the orientation of the polymer chains (molecular axes) coincides with that of one of the crossed polarizers (polarizer axes) the transmitted light is rather weak. This results into four dark perpendicular cones or commonly known as Maltese cross. The light transmission increases as the orientation of the chains makes a non-zero angle with both polarizers, reaching a maximum at 45° (or 135°), which is why the slicing plane for the imaging analysis is typically done at that angle.[2]

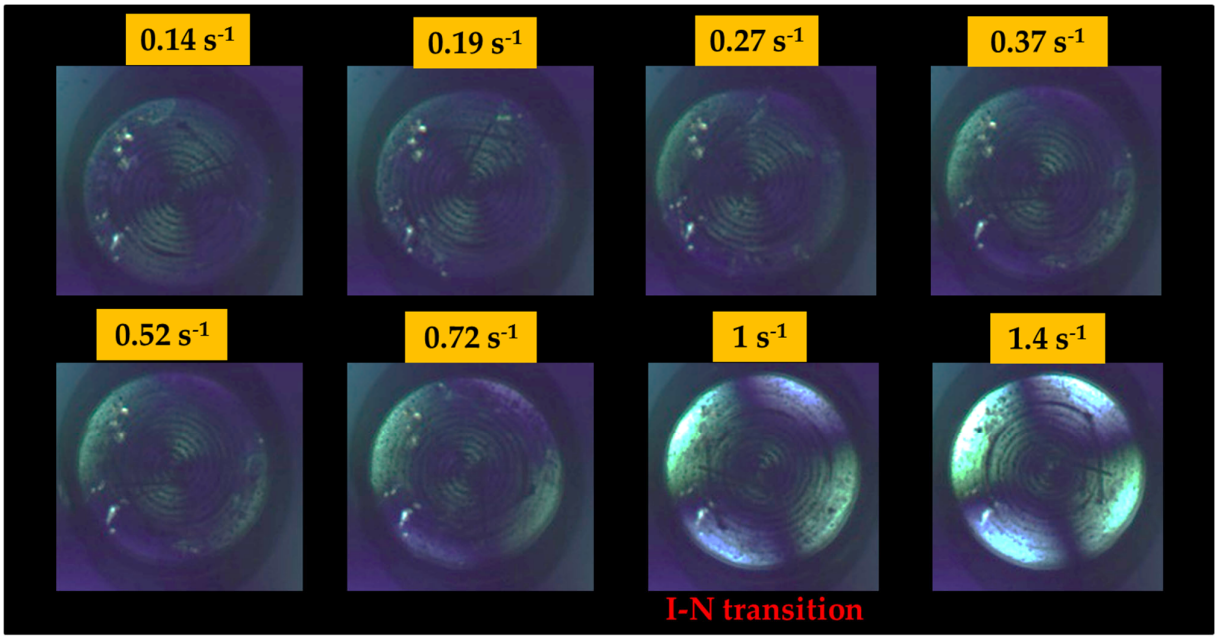

Figure S2. Birefringent images under shear of PEEK 450G at 370 °C. Measurements were performed in a rotational rheometer Anton Paar MCR 502 equipped with a 50 mm diameter transparent quartz bottom plate and an 8 mm diameter polished stainless steel top plate. A reflection polariscope[2,3] was utilized *in situ* as the sample is sheared in the rheometer.

S3. Shear Stress Fluctuations in the Start-up of Shear

Start-up of shear at $\dot{\gamma} = 2\ s^{-1}$ (at the perimeter of the plate) of PEEK 450 G at 370 °C is shown in Figure S3 in terms of apparent viscosity against time. Birefringent images corresponding to the colored symbols in the viscosity data are also reported. $\dot{\gamma} = 2\ s^{-1}$ falls in the region II of the flow curve shown in Figure 1 (see main text). It has been pointed out that, in such a region, the apparent viscosity measured with a plate plate configuration is lower than that measured with the cone partitioned plate (Figure 5 of the main text). A possible conjecture follows. The fixed shearing time based on the lowest shear rate probed in the flow curve ($\dot{\gamma} = 0.01\ s^{-1}$), may not guarantee the steady-state conditions in region II, where two steady-states were observed with the cone partitioned plate. In other words, it is possible that the instrument measures the viscosity during an undershoot of the fluctuations (see Figure S3) underestimating significantly the apparent viscosity. Moreover, with the plate plate geometry the system does not reach a clear second steady-state. Perhaps the shear flow is not homogeneous in a parallel plate geometry as the shear rate varies linearly with the radius, and this might enhance the presence of fluctuations. Finally, as it is known from the literature,[4] the shear-induced nematic strongly depends on shear history, therefore, it is possible that in a shear rate sweep experiment, the polydomain nematic directors experience diverse dynamics because of a different accumulated strain. On the contrary, in start-up of shear experiments, the system always starts from an initial isotropic condition. It is also worth looking at the results in terms of birefringence. Indeed, an unambiguous change in birefringence is observable between the blue, red and purple symbols, when the system undergoes I-N transition. A further increase in time does not seem to change the birefringence pattern significantly, suggesting that the nematic composition is constant but its orientation director is characterized by strong fluctuations, reflected also in the apparent viscosity.

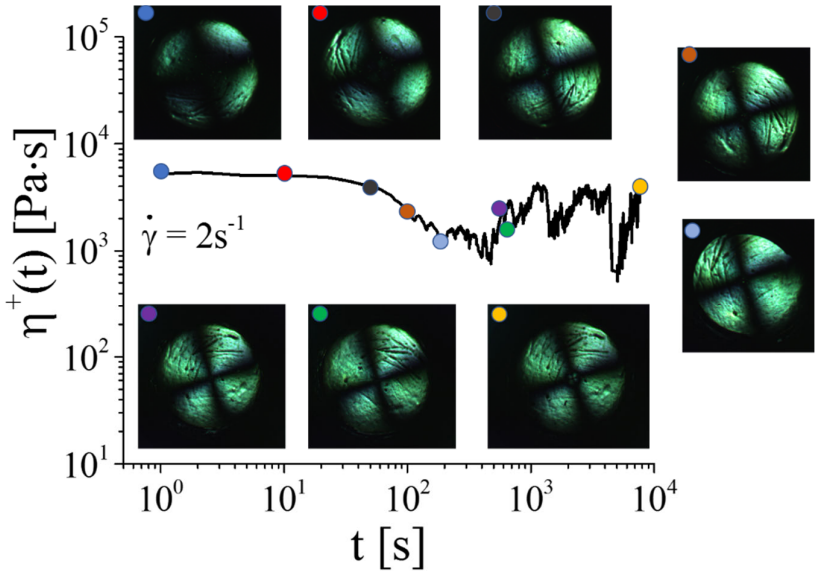

Figure S3. Shear stress growth coefficient as a function of time during start-up of shear flow at 2 s^{-1} (at the perimeter of the plate) for PEEK 450G at 370 °C. Birefringent images at various times, corresponding to the colored circles, are also reported. Measurements were performed in a rotational rheometer Anton Paar MCR 502 equipped with a 50 mm diameter transparent quartz bottom plate and an 8 mm diameter polished stainless steel plate. A reflection polariscope[2,3] was used *in situ* while the sample is sheared in the rheometer.

SI REFERENCES

(1) Nazari, B.; Rhoades, A. M.; Schaake, R. P.; Colby, R. H. Flow-Induced Crystallization of Peek: Isothermal Crystallization Kinetics and Lifetime of Flow-Induced Precursors during Isothermal Annealing. *ACS Macro Letters* **2016**, *5* (7), 849–853.

(2) Mykhaylyk, O. O. Time-Resolved Polarized Light Imaging of Sheared Materials: Application to Polymer Crystallization. *Soft Matter* **2010**, *6* (18), 4430–4440.

(3) Mykhaylyk, O. O.; Warren, N. J.; Parnell, A. J.; Pfeifer, G.; Laeuger, J. Applications of Shear-Induced Polarized Light Imaging (SIPLI) Technique for Mechano-Optical Rheology of Polymers and Soft Matter Materials. *Journal of Polymer Science Part B: Polymer Physics* **2016**, *54* (21), 2151–2170.

(4) Beekmans, F.; Gotsis, A. D.; Norder, B. Influence of the Flow History on Stress Growth and Structure Changes in the Thermotropic Liquid Crystalline Polymer Vectra B950. *Rheologica Acta* **1997**, *36* (1), 82–95.

(5) De Gennes, P.-G.; Prost, J. *The Physics of Liquid Crystals*; Oxford University Press, 1993.

(6) Ugaz, V. M.; Burghardt, W. R. In Situ X-Ray Scattering Study of a Model Thermotropic Copolyester under Shear: Evidence and Consequences of Flow-Aligning Behavior. *Macromolecules* **1998**, *31* (24), 8474–8484.

(7) Ugaz, V. M.; Burghardt, W. R.; Zhou, W.; Kornfield, J. A. Transient Molecular Orientation and Rheology in Flow Aligning Thermotropic Liquid Crystalline Polymers. *Journal of Rheology* **2001**, *45* (5), 1029–1063.

(8) Zhou, W.-J.; Kornfield, J. A.; Burghardt, W. R. Shear Aligning Properties of a Main-Chain Thermotropic Liquid Crystalline Polymer. *Macromolecules* **2001**, *34* (11), 3654–3660.